L.-W. Hung and C. T.-C. Nguyen, "Capacitive-Piezoelectric AlN Resonators With *Q*>12,000," *Tech. Digest*, 24th IEEE Int. Conf. on Micro Electro Mechanical Systems (MEMS'11), Cancun, Mexico, Jan. 24-28, 2011, pp. 173-176.

CAPACITIVE-PIEZOELECTRIC AlN RESONATORS WITH *Q*>12,000

Li-Wen Hung and Clark T.-C. Nguyen
Dept. of EECS, University of California at Berkeley, Berkeley, CA, USA

ABSTRACT

A "capacitive-piezo" transducer that separates a piezoelectric resonator from its electrodes via small gaps to eliminate resonator-to-electrode loss while maintaining strong electromechanical coupling [1], has enabled demonstration of a 50-MHz wine-glass disk (WGD) resonator array with *Q*=12,748. This is higher than exhibited by any sputtered thin-film AlN resonator measured to date at any frequency and more than 2.2× larger than previously achieved by similar devices using conventional (i.e., contacting) electrodes [2]. By attaining such high *Q*, this work erases a common belief that material losses in sputtered AlN dominate the *Q*'s of resonators constructed in this material and confirms that sputtered AlN is a high-*Q* material. It further suggests that energy loss associated with contacting electrodes is primarily responsible for the low *Q*'s of previous AlN resonators. With *Q*'s over 10,000, this work identifies AlN as a viable material for use in channel-selecting RF front ends targeted for future software-defined cognitive radio [3].

INTRODUCTION

Among many transduction methods available to micromechanical resonators, piezoelectric and capacitive transducers, shown in Fig. 1(a) and (b), respectively, have emerged as two of the most promising for future timing and sensing applications. Each has its strengths and weaknesses. Specifically, piezoelectric resonators more readily achieve low motional impedance towards 50Ω, but their lower *Q* (*Q*~3,000) limits performance, particularly the sensitivity of sensors and the insertion loss of narrow-band filters. On the other hand, capacitive resonators readily exhibit *Q*'s larger than 100,000 above 60MHz [4], but suffer from rather large impedances. To achieve simultaneous high *Q* and low impedance, either the *Q* of piezoelectric resonators must be raised, or the impedance of capacitive resonators must be reduced.

Numerous approaches have successfully reduced the impedance of capacitive resonators, among which decreasing their transducer gap spacings seems the most effective. When parallel-plate capacitive transducer gaps shrink below 50nm, however, linearity begins to suffer. For example, using equations for third-order intermodulation input intercept power $PIIP_3$ in [5] as a gauge for resonator linearity, Fig. 2 plots the simulated two-tone (at 600- and 1200-kHz offsets) $PIIP_3$ for 1-GHz 2.7μm-radii 3μm-thick capacitive polysilicon radial-contour mode disk resonators with fully surrounding electrodes [5] and assumed *Q*'s of 100,000 versus gap spacing for DC biases (V_P's) that render 50Ω motional impedance. Here, 10V DC bias and 13.5nm gap spacing yield an impedance of 50Ω and $PIIP_3$ of 18dBm, which exceeds the ~15dBm required by commercial wireless

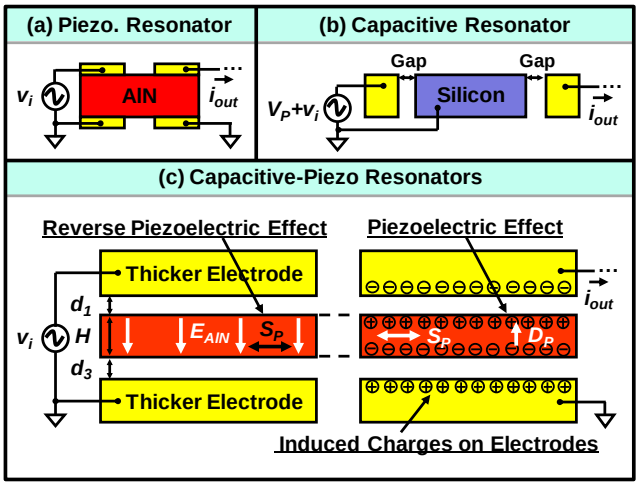

Fig. 1: (a) Conventional piezoelectric resonator employing electrodes that directly contact the piezoelectric structure. (b) Capacitively transduced lateral resonator with gaps separating the resonator and its electrodes. (c) Working principle behind capacitive-piezo transduction. Here, features of (a) and (b) are combined to achieve high coupling (from its piezoelectric component) and high Q (from its non-contacting capacitive component).

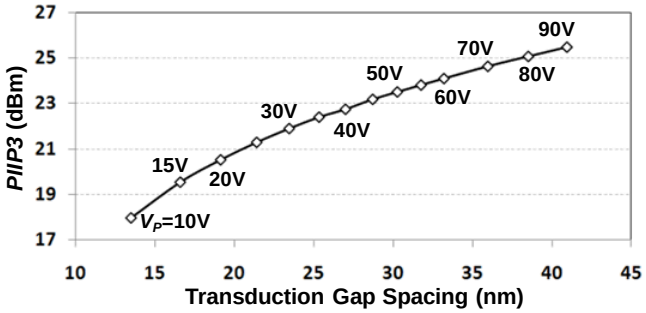

Fig. 2: Simulated $PIIP_3$ versus electrode-to-resonator gap spacing for 1-GHz capacitive polysilicon disk resonators DC-biased to achieve 50Ω motional impedance.

front-ends. To attain higher values, such as needed by more demanding applications, e.g., military, one could couple *n* such resonators into an array-composite like that of [4], which improves the $PIIP_3$ by ~10·log(*n*) dB. If an application requires a $PIIP_3$ >40dBm, one need only increase the array size to >68 resonators with gap spacings relaxed to 38.8nm to maintain a motional impedance of 50Ω. Since disks at 1GHz are very small, the total area of such a 68-resonator array would remain small, on the order of only 71μm × 71μm (with 4μm long coupling beams between resonators). The real question to ponder here is not one of size, but rather whether or not such a large array could be manufactured with high yield.

Piezoelectric resonators, on the other hand, are known for high linear power handling capability in both thickness

(FBAR) modes [6] and contour-modes [7], so need not be assembled into arrays. To overcome their lack of *Q*, [1] very recently demonstrated a "capacitive piezo" transducer that separates a piezoelectric resonator from its electrodes via air gaps to eliminate *Q*-limiting resonator-to-electrode strain loss while maintaining strong electromechanical coupling for low impedance and high linearity. The concept led to a 1.2-GHz AlN resonator with a measured *Q* >3,000, which is higher than achieved by previous GHz range AlN resonators, but still short of prediction due to design limitations. This work incorporates the capacitive-piezo transducer into a higher *Q* wine-glass disk (WGD) design at 50-MHz and achieves *Q*=12,748, which is the highest *Q* measured so far for sputtered AlN resonators at any frequency.

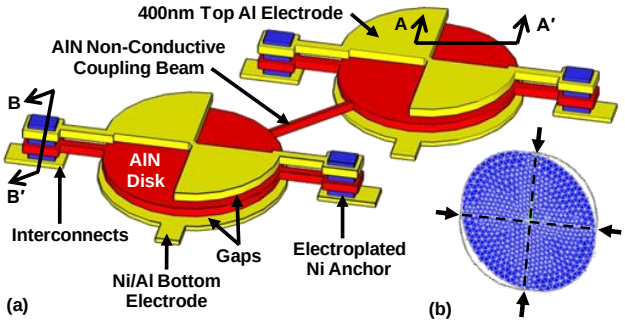

Fig. 3: (a) An array-composite of two AlN disks employing capacitive-piezo transducers with non-contacting electrodes, drawn with exaggerated vertical gaps. The top electrodes are patterned for wine-glass mode resonance, for which quasi-nodal points can be accessed on the edges, as shown in (b).

THE CAPACITIVE-PIEZO TRANSDUCER

Fig. 1(c) presents a cross-section describing the basic structure and concept behind the capacitive-piezo transducer of [1]. Here, instead of attaching the electrodes directly to the resonant piezoelectric structure as done in (a), the electrodes are separated from the structure, but in very close proximity. Typical electrode-to-resonator gaps are on the order of only 100nm in order to maintain strong electric fields through the piezoelectric material sandwiched between the top and bottom electrodes. If the gap spacing is small, only a small amount of electromechanical coupling is lost versus the case where electrodes attach to the structure—a very small price to pay considering the *Q* benefits that ensue.

Indeed, due to the historically lower *Q*'s (by 20×) measured on previous AlN resonators than on silicon ones, popular opinion stipulates that sputtered AlN thin films are inherently low *Q* materials. However, material loss theory predicts that the material *Q* of AlN should only be around two times lower than that of silicon [8]. The capacitive-piezo transducer of Fig. 1(c) presupposes that theory is correct—i.e., that AlN is a high *Q* material—and that the metal electrodes are the main culprit limiting the *Q*. In particular, electrodes in contact with the piezoelectric material may dissipate energy in numerous ways, from direct strain coupling of the resonator to its lossy metal electrodes [9], to interface thermoelastic dissipation (TED) [10], to hysteretic movement of electrode-to-resonator interface defects [11].

Separating the electrodes from the piezoelectric resonator not only eliminates the above loss mechanisms, but in so doing also obviates previous constraints on electrode thickness imposed to lessen electrode-based mechanical losses. This then permits the use of much thicker electrodes, which in turn reduces electrode resistance, further enhancing the *Q* of the total device. This is especially important for high frequency devices with scaled lateral dimensions that constrain the electrode routing area. All things considered, the use of a capacitive-piezo transducer has the potential to reveal the true *Q* of a given piezoelectric material, sans any influence from electrodes.

TAPPING THE MATERIAL *Q* OF ALN

Unfortunately, the work of [1] did not expose the intrinsic material *Q* of AlN. In particular, although the *Q* of 3,073 measured in [1] on a 1.2-GHz capacitive-piezo contour-mode ring resonator is higher than any reported previously, it is much more likely that anchor losses, not material losses, had the strongest role in dictating the *Q*. The main culprits were fabrication limitations that prevented attachment of supports at the nodal circle of the ring located at the midpoint of its width [12]. At the nodal circle, there are ideally no radial displacements, so attachment at this line minimizes induced motions in the support, which in turn minimizes energy loss to anchors. Unfortunately, multiple reflective metal layers and heavy undercutting of the top metal layer in the fabrication process of [1] significantly complicated lithography, making it difficult to produce the ring notches needed for supports to attach at the nodal circle. The inability to attain notched supports led to excessive anchor loss that dominated the *Q*.

The present work circumvents this problem by using the disk geometry shown in Fig. 3(a) that vibrates in the wine-glass mode shape shown in Fig. 3(b), in which the disk expands and contracts in opposite directions along orthogonal axes. In this mode shape, nodal lines shown in Fig. 3(b) are accessible at points along the disk edge, obviating the need for notches and facilitating achievement of a *Q*-optimized design that can better expose the intrinsic material *Q* of AlN.

It should be mentioned that the wine-glass mode shape used here that facilitates *Q*-optimization also generates longitudinal and shear strains that are out-of-phase, thereby making it difficult to excite and sense the mode using the piezoelectric effect. Thus, although the devices of this work are good vehicles for tapping the *Q* of sputtered AlN, they are not so suitable for attaining low impedance. This also means that their output currents will be small, so will not be easy to measure in the presence of feedthrough signals.

To simplify measurement, this work employs half-wavelength coupled arrays [4] of disks, such as shown in Fig. 3(a). Here, uniform bottom and patterned top electrodes are spaced 260nm from the top and underside, respectively, of each AlN disk. The top electrodes make electrical contact to substrate interconnects through vias at the anchors. As detailed in [4], half-wavelength coupling effectively converts

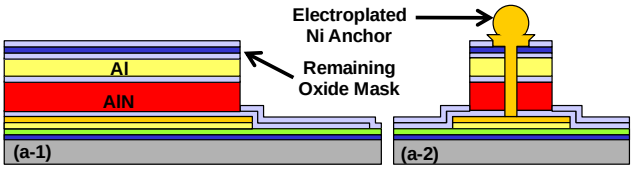

(a) Achieved using a series of sputtering, lift-off, etching, electroplating, and seven lithography steps

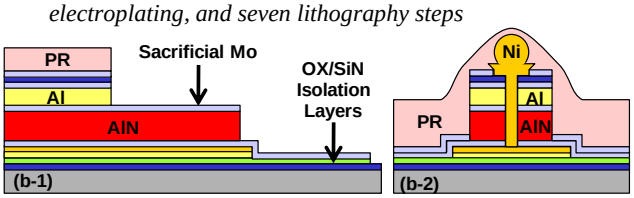

(b) Cross-section after patterning top electrodes for wine-glass mode resonance by etching away the film stacks of Mo/Oxide/Mo/Al. The etch stops on the sacrificial Mo layer.

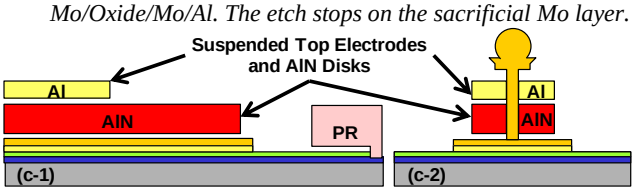

(c) Achieved after covering the exposed nitride isolation layer with PR, removing the remaining oxide mask, and releasing using a mixture of XeF_2/N_2 gases.

Fig. 4: Cross-sections along A-A′ and B-B′ in Fig. 3(a) summarizing the last few steps of the fabrication process flow.

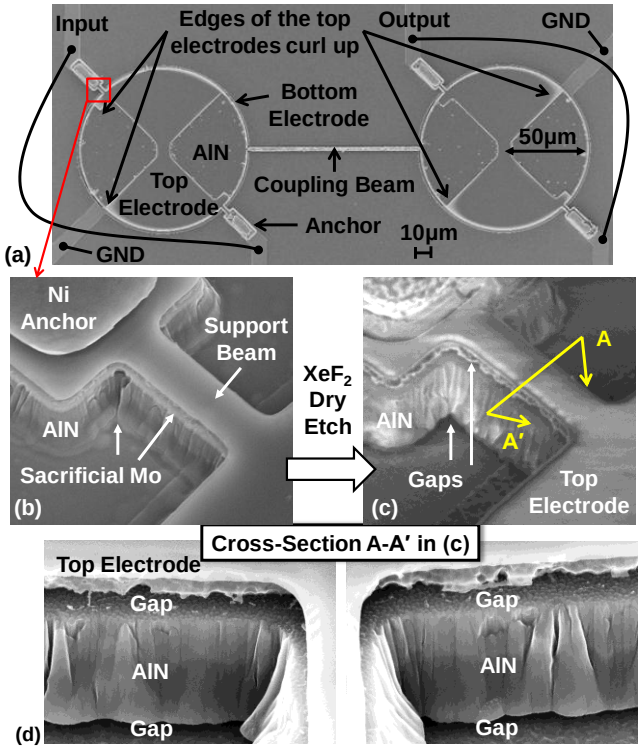

Fig. 5: SEMs of (a) a fabricated AlN 2-disk array-composite with zoom-ins on an anchor (b) before and (c) after XeF_2 dry release. (d) Zoom-in SEM on the gaps generated after release.

this device into a single composite device where constituent resonators vibrate together at one mode frequency, with little or no reduction in the overall *Q* of this mechanical circuit relative to that of a stand-alone device. The use of two devices in this mechanical circuit makes available two ports for interrogation: an input port to drive the device, and an output port to sense its motion, both separated by a non-conductive AlN coupling beam that blocks feedthrough current, thereby greatly facilitating evaluation of piezoelectric wine-glass disks.

DEVICE FABRICATION

Fig. 4 presents cross-sectional views of a capacitive-piezo wine-glass disk resonator at different steps during its fabrication. The process for these devices mimics that required to achieve the device of [1] up to the step of electroplating nickel anchors, at which point the cross-section is as shown in Fig. 4(a). It then deviates from the previous process by patterning the top electrodes on the AlN disks, etching them and stopping on the molybdenum layer between AlN and Al top electrodes, shown in Fig. 4(b). This step requires that Mo and Al be dry etched one after the other, and this is done using Cl_2-based chemistries with varying amounts of added O_2 that alter etch selectivities. After another lithography step to cover any exposed nitride isolation layer and another dry etch to remove the remaining oxide mask above the remaining Al films, the resonators are baked at 120°C for 20 minutes to dehydrate the wafers as much as possible, then released in a mixture of XeF_2/N_2 gases, to yield the cross-section of Fig. 4(c). The dehydration bake prevents moisture from forming HF during the XeF_2 dry release etch, which effectively enhances the etch selectivity of molybdenum over oxide and nitride isolation layers. Such high etch selectivity is necessary to release 50µm-radius disks suspended 260nm above the substrate.

Fig. 5(a) presents the overhead SEM of a fabricated capacitive-piezo two-disk array-composite resonator. Fig. 5(b) and (c) show zoom-in views on the anchoring areas before and after release, respectively, clearly showing that the Al top electrode and the AlN structural layer are supported by electroplated nickel anchors after removing the sacrificial molybdenum layer. Fig. 5(d) further presents zoom-in views of the A-A′ cross-section in Fig. 5(c), showing 260nm gaps both above and under the AlN disk between the electrodes.

EXPERIMENTAL RESULTS

Fig. 5(a) presents the set-up used to measure the frequency characteristics for two-disk array-composites. Here, the bottom electrodes of both resonators are grounded, while an AC input signal is applied to the top electrode of the left device and the output taken from that of the right. Although they possess AC signals, the input and output electrodes are DC grounded to prevent large electrostatic forces from pulling the electrodes into contact with the AlN disks.

Fig. 7(a) presents measured frequency characteristics for two-disk array composite resonators employing various support beam widths (c.f., Fig. 6) measured immediately

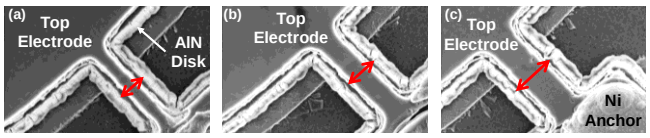

Fig. 6: Zoom-in SEMs of the support beams used in this work with various widths: (a) 1 µm; (b) 1.5 µm; (c) 2 µm.

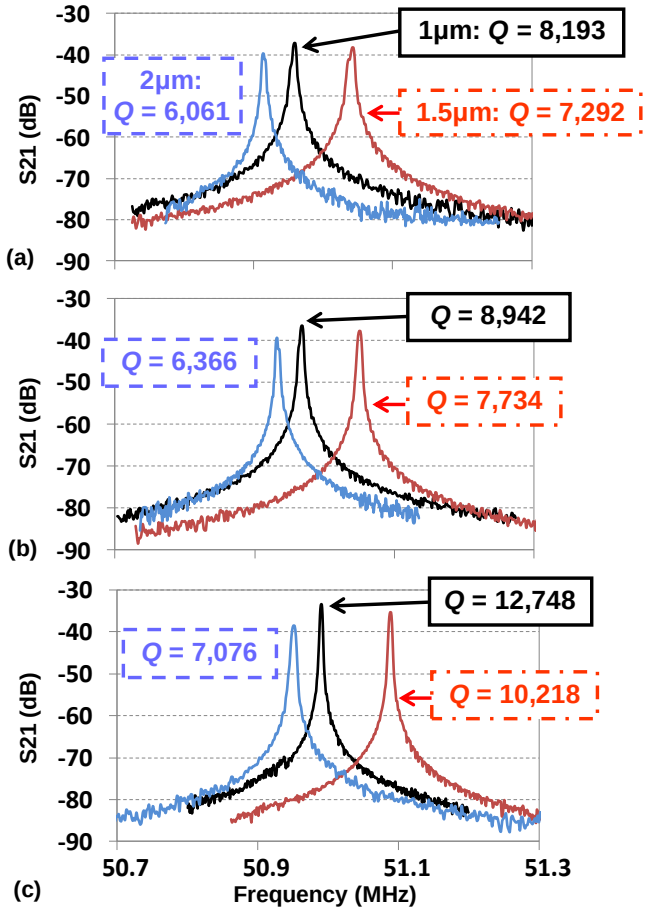

Fig. 7: Measured frequency characteristics for the resonator of Fig. 5 after each cleaning and anneal procedure: (a) as released; (b) after O_2 plasma clean, EKC-270 dip, and critical point drying; and (c) after annealing at 300°C in forming gas for 30 minutes, achieving the highest Q of 12,748, which is the highest ever measured for any sputtered AlN resonator. That resonators with thinner support beams attain the highest Q indicates that anchor loss still dominates the Q, even for these wine-glass disks.

after XeF_2 release, with the photoresist protecting nitride/oxide isolation layers during the release still present on the chip. Here, resonators with support beam widths of 1µm, 1.5µm, and 2µm, exhibit *Q*'s of 8,193, 7,292, and 6,061, respectively. After removing photoresist via O_2 plasma etching, then dipping in EKC-270 and performing critical point drying, *Q*'s increase for all three cases, as shown in Fig. 7(b), up to a high of 8,942 for the 1µm-wide support version. The observed increase emphasizes the importance of cleanliness to maximize *Q*.

A following anneal in N_2/H_2 at 500°C for 30 minutes further raises *Q* to a high of 12,748 (again, for the 1µm-wide support version), posting the highest *Q* ever measured for sputtered thin-film AlN resonators. The mechanism behind this anneal-based increase in *Q* is presently under study. Possible mechanisms include burning off of etch residuals or contaminants, strengthening or stress relaxation in the nickel anchor pegs, and changes in AlN material, e.g., stress relaxation.

The fact that the 1µm-wide support beam version exhibits the highest *Q* after each cleaning/annealing procedure indicates that anchor losses still influence the *Q*, but much less so than in [1], allowing measurement of much higher *Q* in this work. Thus, it is likely that the *Q* of AlN is actually higher than the 12,748 measured here, as would be predicted by theory.

CONCLUSIONS

By applying capacitive-piezo transduction to separate a 50-MHz AlN two-disk array-composite resonator from its electrodes by nano-scale gaps, a *Q* as high as 12,748 has been measured, which is the highest measured so far for any AlN resonator. The results of this work experimentally confirm theoretical predictions that AlN is a high *Q* material, capable of achieving the *Q* >10,000 needed for some RF channel-select wireless communication front-ends. They also confirm that it is most likely electrode loss, not material loss that dictates the lower *Q*'s previously measured for AlN resonators with contacting electrodes. Given evidence that anchor losses probably still dominate the *Q*'s of the devices used in this work, it would not be surprising if future use of capacitive-piezo transduction in more effective anchor-isolating designs yields devices with even higher *Q*'s. Work towards this continues.

***Acknowledgment*:** This work was funded by DARPA.

REFERENCES

[1] L.-W. Hung and C. T.-C. Nguyen, "Capacitive-piezo transducers for higher *Q* contour-mode…," *Hilton Head*, 2010, pp. 463-466.

[2] G. Piazza, *et. al.*, "Piezoelectric aluminum nitride vibrating contour…," *J. Microelectromech. Syst.*, vol. 15, pp. 1406-1418, 2006.

[3] C. T.-C. Nguyen, "Integrated micromechanical RF...," 26th *Sensors, Micromachines & App. Sys. Sym.*, 2009, pp. 1-5.

[4] Y.-W. Lin, *et. al.*, "Low phase noise array-composite micromechanical wine-glass disk oscillator," *IEDM'05*, pp. 287-290.

[5] Y.-W. Lin, *et. al.*, "Third-order intermodulation distortion…," *Proc., IEEE Int. Ultrasonics Sym.*, 2005, pp. 1592-1595.

[6] J. D. Larson, *et. al.*, "Power handling and temperature coefficient studies…," *Proc., IEEE Int. Ultrasonics Sym.*, 2000, pp. 869-874.

[7] Z. Chengjie, *et. al.*, "Power handling and related frequency scaling…," *Proc., IEEE Int. Ultrasonics Sym.*, 2009, pp. 1187-1190.

[8] R. Tabrizian, *et. al.*, "Effect of phonon interactions on limiting the *f*·*Q* product of micromechanical…," *Transducers'09*, pp. 2131-2134.

[9] C. G. Courcimault and M. G. Allen, "High-*Q* mechanical tuning tuning of MEMS resonators…," *Transducers'05*, pp. 875-878.

[10] S. Vengallatore, "Analysis of thermoelastic damping in laminated…," *J. Micromech. Microeng.*, vol. 15, pp. 2398–2404, 2005.

[11] J. R. Vig and T. R. Meeker, "The aging of bulk acoustic wave resonators...," *Proc., IEEE Freq. Control Sym.*, 1991, pp. 77-101.

[12] S.-S. Li, *et. al.*, "Micromechanical "hollow-disk" ring resonators," *Proceedings, MEMS'04,* pp. 821-824.